A Novel Bi-Hemispheric Discrepancy Model for EEG Emotion Recognition

Yang Li, *Member, IEEE*, Lei Wang, *Senior Member, IEEE*, Wenming Zheng, *Senior Member, IEEE*, Yuan Zong, *Member, IEEE*, Lei Qi, Zhen Cui, *Member, IEEE*, Tong Zhang, *Member, IEEE*, and Tengfei Song, *Member, IEEE*

***Abstract*—Neuroscience study has revealed the discrepancy of emotion expression between the left and right hemispheres of human brain. Inspired by this study, in this article, we propose a novel bi-hemispheric discrepancy model (BiHDM) to learn this discrepancy information between the two hemispheres to improve electroencephalograph (EEG) emotion recognition. Concretely, we first employ four directed recurrent neural networks (RNNs) based on two spatial orientations to traverse electrode signals on two separate brain regions. This enables the proposed model to obtain the deep representations of all the EEG electrodes' signals that keep their intrinsic spatial dependence. Upon this representation, a pairwise subnetwork is designed to explicitly capture the discrepancy information between the two hemispheres and extract higher level features for final classification. Furthermore, considering the presence of the domain shift between training and testing data, we incorporate a domain discriminator that adversarially induces the overall feature learning module to generate emotion related but domain-invariant feature representation so as to further promote EEG emotion recognition. Experiments are conducted on three public EEG emotional data sets, in which we evaluate the performance of the proposed BiHDM as well as investigated the important brain areas in emotion expression and explore to use less electrodes to achieve comparable results. These experimental results jointly demonstrate the effectiveness and advantage of the proposed BiHDM model in solving the EEG emotion recognition problem.**

***Index Terms*—Bi-hemispheric discrepancy model (BiHDM), electroencephalograph (EEG), EEG emotion recognition.**

Manuscript received June 17, 2019; revised December 15, 2019 and March 6, 2020; accepted April 23, 2020. Date of publication June 1, 2020; date of current version June 10, 2021. This work was supported in part by the National Key Research and Development Program of China under Grant 2018YFB1305200; in part by the National Natural Science Foundation of China under Grant 61921004, Grant 61906094, Grant 61772276, Grant 61902064, and Grant 81971282; in part by the Natural Science Foundation of Jiangsu Province under Grant BK20190452 and Grant BK20192004; and in part by the Fundamental Research Funds for the Central Universities under Grant 2242018K3DN01. *(Corresponding author: Wenming Zheng.)*

Yang Li is with the Key Laboratory of Child Development and Learning Science (Ministry of Education) and the Department of Information Science and Engineering, Southeast University, Nanjing 210096, China, and also with the Key Laboratory of Intelligent Perception and Image Understanding of Ministry of Education and the School of Artificial Intelligence, Xidian University, Xi'an 710071, China.

Lei Wang is with the School of Computing and Information Technology, University of Wollongong, Wollongong, NSW 2500, Australia.

Wenming Zheng and Yuan Zong are with the Key Laboratory of Child Development and Learning Science (Ministry of Education), School of Biological Sciences and Medical Engineering, Southeast University, Nanjing 210096, China (e-mail: wenming_zheng@seu.edu.cn).

Lei Qi is with the State Key Laboratory for Novel Software Technology, Nanjing University, Nanjing 210096, China.

Zhen Cui and Tong Zhang are with the School of Computer Science and Engineering, Nanjing University of Science and Technology, Nanjing 210096, China.

Tengfei Song is with the Key Laboratory of Child Development and Learning Science (Ministry of Education) and the Department of Information Science and Engineering, Southeast University, Nanjing 210096, China.

Color versions of one or more figures in this article are available at https://doi.org/10.1109/TCDS.2020.2999337.

Digital Object Identifier 10.1109/TCDS.2020.2999337

I. Introduction

EMOTION, as a common mental phenomenon, is closely related to our daily life. Although it is easy to sense other people's emotion in human–human interaction, it is still difficult for machines to understand the complicated emotions of human beings [2]. As the key step to make machines capture human emotions, emotion recognition has received substantial attention from human–machine interaction (HMI) and pattern recognition communities in recent years [3]–[5].

Human emotional expressions are mostly based on verbal behavior methods (e.g., speech) and nonverbal behavior methods (e.g., facial expression). Therefore, a large body of literature concentrates on learning the emotional components from speech and facial expression data. However, from the viewpoint of neuroscience, human's emotion originates from a variety of brain cortex regions, such as the orbital frontal cortex, ventral medial prefrontal cortex, and amygdala [6], which provides us a potential approach to decoding emotion by recording the continuous brain activity signals over these regions. For example, by placing the electroencephalograph (EEG) electrodes on the scalp, we can record the neural activities in the brain, and they can be used to recognize human emotions.

Most existing EEG emotion recognition methods focus on two fundamental challenges. One is how to extract discriminative features related to emotions. Typically, EEG features can be extracted from the time domain, frequency domain, and time-frequency domain. Jenke *et al.* [7] evaluated all the existing features by using machine learning techniques on a self-recorded data set. The other challenge is how to classify the features correctly. Many EEG emotion recognition models and methods have been proposed over the past years [8], [9]. For example, Zheng [10] proposed a group sparse canonical correlation analysis (GSCCA) method for simultaneous EEG channel selection and emotion recognition. Li *et al.* [11] fused the information propagation patterns and activation difference in the brain to improve emotional recognition.

Although various methods have been proposed for EEG emotion recognition, the performance is still far from

satisfactory. By looking into the literature, we argue that the following two issues need to be better addressed. The first one is how to extract the features that are specific with emotions. A typical example is the handcrafted features, such as statistical measure, power spectrum density (PSD), and discrete wavelet transform, which are frequently used for generic EEG signal classification tasks rather than specially designed for EEG emotion recognition. This issue has also appeared in some recent deep learning researches for EEG emotion recognition, such as the work by Zheng and Lu [12], which uses the deep belief network (DBN) to directly model the EEG emotion signal. Even though these handcrafted and deep features have been able to extract certain emotion discriminative information, they have not sufficiently exploited the specific emotion-related information in EEG emotion recognition tasks. In other words, it will be more promising and fruitful if we can integrate the unique characteristics of EEG emotion signals into machine learning algorithms to extract better emotion-related features. It is well realized through neuroscience study that although the anatomy of human brain looks symmetric, the left and right hemispheres have different responses to emotions. From the view of neuroscience, Dimond *et al.* [1], Davidson *et al.* [13], and Herrington *et al.* [14] have studied the asymmetry of emotion expression; meanwhile Schwartz *et al.* [15], Wager *et al.* [16], and Costanzo *et al.* [17] have discussed the emotion lateralization. The discrepancy property of two brain hemispheres is just a kind of emotion-specific information by exploiting which we expect to obtain more discriminative information to recognize the EEG emotion signals.

The second major issue for EEG emotion recognition is how to improve the generalization. Since EEG emotional signal usually consists of many neural processes, it presents a highly heterogeneous and nonstationary behavior [9]. This leads to a lack of generalization to new data. A typical example is the cross-subject (subject-independent) EEG emotion recognition task, in which the training and testing EEG data are from different subjects hence there exists a potential data distribution shift between them. Narrowing this shift will further improve EEG emotion recognition and the generalization to new EEG emotional data. Recently, deep learning techniques have shown significant improvement in various pattern recognition applications, such as face recognition [18], image classification [19], and speech recognition [20]. Especially, the domain adversarial neural network (DANN) [21], which uses a domain discriminator to alleviate the differences of the feature distribution between the source domain and the target domain, has shown its ability in dealing with the domain adaptation problem. It will be helpful to utilize this technique for the cross-domain EEG emotion recognition problem.

To address the above two major issues in EEG emotion recognition tasks, in this article, we propose a novel neural network model bi-hemispheric discrepancy model (BiHDM) to learn the bi-hemispheric discrepancy information in EEG emotion signals, and meanwhile, try to reduce the potential domain gaps between source and target domains so as to improve the generality of the model for EEG emotion recognition. To achieve the first goal, we need to solve two major problems, i.e., how to extract the features for each hemispheric EEG data and then measure the difference between them. The EEG data consist of several electrodes that are set under the coordinates on the scalp, which are predefined referring to the locations of different brain areas. In the feature learning procedure of each hemisphere, we should well retain this intrinsic structural information of EEG data. We can achieve this by using the horizontal and vertical traversing recurrent neural networks (RNNs), which will construct a complete relationship and generate discriminative deep features for all the EEG electrodes. After obtaining these deep features of each electrode, we can extract the asymmetric discrepancy information between two hemispheres by performing specific pairwise operations for paired symmetric electrodes. The second goal is to ensure that the extracted EEG features are robust to the domain gaps. We can achieve this by leveraging a domain discriminator that works cooperatively with the classifier to produce the emotion related but domain-invariant data representation.

To the best of our knowledge, this is the first work to exploit the bi-hemispheric discrepancy relation for deep learning models to improve EEG emotion recognition. The experimental results verify the discrimination and effectiveness of this differential information between the left and right hemispheres. Besides, we also try to identify which electrodes are more tightly associated with emotion recognition, explore how to select a small number of electrodes while maintaining recognition performance, and further investigate which hemisphere is more correlated with emotion recognition.

The remainder of this article is organized as follows. Section II reviews some related works in EEG emotion recognition. Section III specifies the method of BiHDM as well as its application to EEG emotion recognition. In Section IV, extensive experiments are conducted to evaluate the proposed method for EEG emotion recognition. Sections IV-C and V discuss this article and conclude it.

II. Related Works

A. Existing Methods That Considered the Difference of Emotion Expression Between Two Hemispheres

In the past years, many researchers have attempted to utilize the difference between left and right hemispheres as prior knowledge to extract features or develop models, effectively enhancing the performance of EEG emotion recognition. For example, Hinrikus *et al.* [22] used EEG spectral asymmetry index for depression detection. Lin *et al.* [4] investigated the relationships between emotional states and brain activities, and extracted PSD, differential asymmetry power, and rational asymmetry power as features. Motivated by their previous findings of critical brain areas for emotion recognition, Zheng *et al.* [5] selected six symmetrical temporal lobe electrodes as the critical channels and propose a network called EmotionMeter to model EEG emotional signal. Li *et al.* [23] proposed a novel neural network called BiDANN that separately extracted two brain hemispheric features and achieved the state-of-the-art classification performance. The above literature demonstrates that some researchers have realized the significance of the difference between the left and right hemispheres for EEG emotion recognition. Since how to utilize the

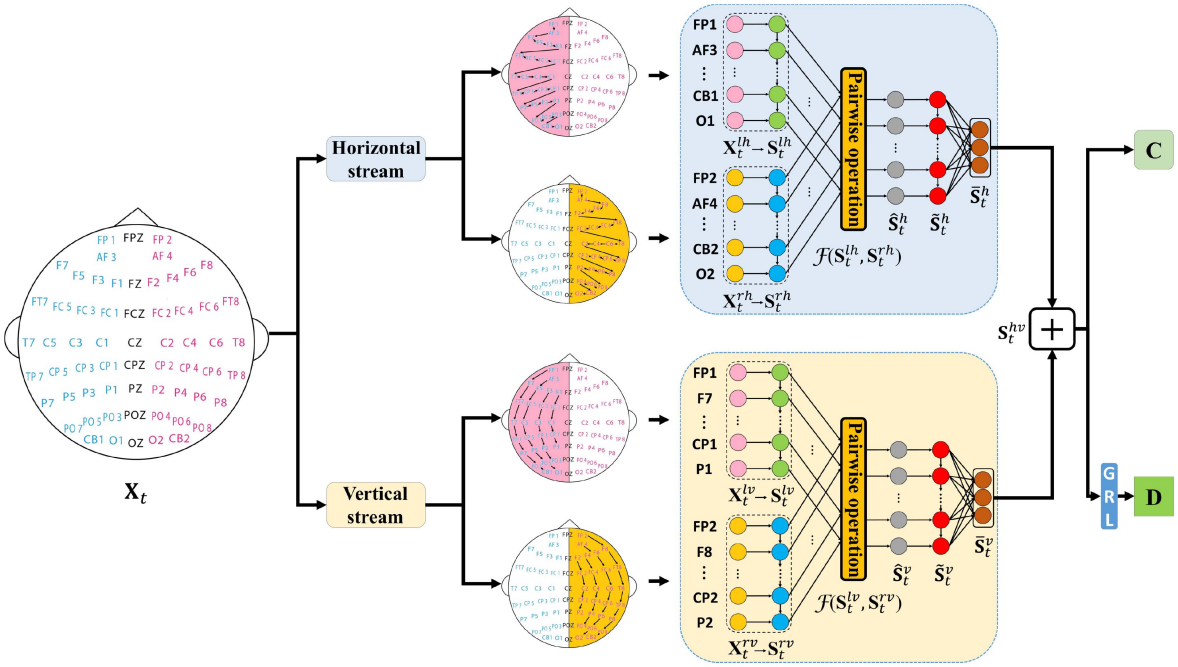

Fig. 1. Framework of BiHDM. BiHDM consists of four RNN modules to capture the information of EEG electrodes on each hemisphere from horizontal and vertical streams. Then all the deep representations of the electrodes are fed into the discrepancy extracting module to form the final vector for the classifier and discriminator.

characteristics of EEG emotional signal is a challenging topic in EEG emotion recognition area, explicitly extracting the discrepancy between two brain hemispheres by deep learning models will be meaningful and further improve EEG emotion recognition, and will be explored in this article.

B. Other Existing Methods for EEG Emotion Recognition

Various machine learning methods have been proposed to solve EEG emotion recognition in the literature. For example, Zheng [10] proposed a GSCCA method for simultaneous EEG channel selection and emotion recognition. Li *et al.* [24] proposed a graph regularized sparse linear regression (GRSLR) method to deal with EEG emotion recognition. Recently, using deep learning methods for EEG emotion recognition has been increasingly adopted and demonstrated better performance than traditional methods. Zheng and Lu [12] proposed to use DBN for EEG emotion classification. Zhang *et al.* [25] employed a multidirectional RNN layer to capture long-range contextual cues by traversing the spatial regions of each temporal slice along different directions. Song *et al.* [26] used the dynamic graph convolution neural network (DGCNN) to model the multichannel EEG features and they also presented a novel attention-long short-term memory (A-LSTM) [27] which strengthens the effectiveness of useful sequences to extract more discriminative features. However, these existing methods only model the relation between EEG signals and the emotion class labels to obtain the deep features. It is better to concentrate on capturing the emotion-specific information, which is more important and will improve EEG emotion recognition. We will compare the proposed methods with the aforementioned ones in the experimental study.

III. Proposed Model for EEG Emotion Recognition

To specify the proposed method clearly, we illustrate the framework of the BiHDM model in Fig. 1. Its goal is to capture the asymmetric differential information between two hemispheres. We adopt three steps to achieve this goal. The first step is to obtain the deep representations of all the electrodes' data. Subsequently, the relationship is characterized between the identified paired electrodes on two hemispheres, and hence a more discriminative and higher level discrepancy feature is generated for final classification. Third, a classifier and a discriminator are leveraged to cooperatively induce the above process to generate the emotion related but domain-invariant features. The overall process is described as follows.

A. Obtaining the Deep Representation for Each Electrode

Note that EEG signals can be treated as a set of sequences since the dimensions of all the electrodes are same. For this reason, the EEG data can be fed into the RNN module to extract high-level deep features, which will contain the spatial relation information. In BiHDM, we separately extract the EEG electrodes' deep features on the left and right brain hemispheres by using two independent RNN modules. Meanwhile, to consider the intrinsic structural information of EEG data that reflects the relations between brain regions, for each hemispheric EEG data, we build the RNN module traversing the spatial regions under two predefined stacks, which are determined with respect to horizontal and vertical directions. These two directional RNNs are complementary to construct a complete relationship of electrodes' locations. Concretely, for an EEG sample $\mathbf{X}_t$, it is split as $\mathbf{X}_t = [\mathbf{X}_t^l, \mathbf{X}_t^r] = [\mathbf{x}_1^l, \ldots, \mathbf{x}_{(N/2)}^l, \mathbf{x}_1^r, \ldots, \mathbf{x}_{(N/2)}^r] \in \mathbb{R}^{d \times N}$, where $\mathbf{X}_t^l$ and $\mathbf{X}_t^r$

denote the EEG electrodes' data on the left and right hemispheres, d is the dimension of each EEG electrode's data, and N is the number of electrodes. When modeling spatial dependencies, we traverse through the electrodes on two hemispheres separately with a predefined forward evolution sequence so that the input state and the previous states can be defined for an RNN unit. This process can be formulated as

$$\mathbf{s}_i^l = \sigma\left(\mathbf{U}^l\mathbf{x}_i^l + \sum_{j=1}^{N/2} e_{ij}^l\mathbf{V}^l\mathbf{s}_j^l + \mathbf{b}^l\right) \in \mathbb{R}^{d_l\times 1} \tag{1}$$

$$\mathbf{s}_i^r = \sigma\left(\mathbf{U}^r\mathbf{x}_i^r + \sum_{j=1}^{N/2} e_{ij}^r\mathbf{V}^r\mathbf{s}_j^r + \mathbf{b}^r\right) \in \mathbb{R}^{d_r\times 1} \tag{2}$$

$$e_{ij}^{\cdot} = \begin{cases} 1, & \text{if } \mathbf{x}_j^{\cdot} \in \mathcal{N}\left(\mathbf{x}_i^{\cdot}\right) \\ 0, & \text{otherwise} \end{cases} \tag{3}$$

where $\mathbf{s}_i^l$, $\mathbf{s}_i^r$ and d_l, d_r are the hidden units and the dimensions of RNN modules on the left and right hemispheres, respectively; $\sigma(\cdot)$ denotes the nonlinear operation, such as the sigmoid function; $\{\mathbf{U}^l \in \mathbb{R}^{d_l\times d}, \mathbf{V}^l \in \mathbb{R}^{d_l\times d_l}, \mathbf{b}^l \in \mathbb{R}^{d_l\times 1}\}$ and $\{\mathbf{U}^r \in \mathbb{R}^{d_r\times d}, \mathbf{V}^r \in \mathbb{R}^{d_r\times d_r}, \mathbf{b}^r \in \mathbb{R}^{d_r\times 1}\}$ are the learnable transformation matrices of the two hemispheric RNN modules; and $\mathcal{N}(\mathbf{x}_i^{\cdot})$ denotes the set of predecessors of the node $\mathbf{x}_i^{\cdot}$. Here, $d_l = d_r$. As the RNN modules traverse all the nodes, the obtained hidden states $\mathbf{s}_i^l$ and $\mathbf{s}_i^r$ can be used as the deep features to represent the ith electrode's data on two hemispheres.

Particularly, for the left and right hemispheric RNN modules, they traverse the spatial regions under two predefined horizontal and vertical stacks. Therefore, we will obtain two paired deep feature sets, i.e., $(\mathbf{S}_t^{lh}, \mathbf{S}_t^{rh})$ and $(\mathbf{S}_t^{lv}, \mathbf{S}_t^{rv})$, where $\mathbf{S}_t^{lh} = \{\mathbf{s}_i^{lh}\} \in \mathbb{R}^{d_l\times(N/2)}$ and $\mathbf{S}_t^{rh} = \{\mathbf{s}_i^{rh}\} \in \mathbb{R}^{d_r\times(N/2)}$ represent the deep features of left and right hemispheric electrodes under horizontal direction, while $\mathbf{S}_t^{lv} = \{\mathbf{s}_i^{lv}\} \in \mathbb{R}^{d_l\times(N/2)}$ and $\mathbf{S}_t^{rv} = \{\mathbf{s}_i^{rv}\} \in \mathbb{R}^{d_r\times(N/2)}$ represent the deep features under vertical direction. So far, we obtain the deep representation of each electrode which meanwhile keeps the location structural relation.

B. Interaction Between the Paired Electrodes on Two Hemispheres

After obtaining the deep features of every electrode, to identify the asymmetric differential information between two hemispheres, we perform a specific pairwise operation on the paired electrodes referring to the symmetric locations on the brain scalp. This operation can be expressed as

$$\hat{\mathbf{S}}_t^h = \mathcal{F}\left(\mathbf{S}_t^{lh}, \mathbf{S}_t^{rh}\right) = \mathcal{F}\left(\left\{\mathbf{s}_i^{lh}\right\}, \left\{\mathbf{s}_i^{rh}\right\}\right) \in \mathbb{R}^{d_p\times(N/2)} \tag{4}$$

$$\hat{\mathbf{S}}_t^v = \mathcal{F}\left(\mathbf{S}_t^{lv}, \mathbf{S}_t^{rv}\right) = \mathcal{F}\left(\left\{\mathbf{s}_i^{lv}\right\}, \left\{\mathbf{s}_i^{rv}\right\}\right) \in \mathbb{R}^{d_p\times(N/2)} \tag{5}$$

where $\hat{\mathbf{S}}_t^h = \{\hat{\mathbf{s}}_i^h\}$ and $\hat{\mathbf{S}}_t^v = \{\hat{\mathbf{s}}_i^v\}$ are the deep asymmetric differential features, and $\mathcal{F}(\cdot)$ denotes the pairwise operation between the data representation of two paired electrodes. Concretely, for each paired data $(\mathbf{s}_i^{l\cdot}, \mathbf{s}_i^{r\cdot})$, we apply subtraction, division, and inner product on it, which can be formulated as

$$\mathcal{F}\left(\left\{\mathbf{s}_i^{l\cdot}\right\}, \left\{\mathbf{s}_i^{r\cdot}\right\}\right) = \begin{cases} \left\{\mathbf{s}_i^{l\cdot} - \mathbf{s}_i^{r\cdot}\right\} \in \mathbb{R}^{d_{p_1}\times\frac{N}{2}} \\ \left\{\mathbf{s}_i^{l\cdot}/\mathbf{s}_i^{r\cdot}\right\} \in \mathbb{R}^{d_{p_2}\times\frac{N}{2}} \\ \left\{s_{i,1}^{l\cdot}\cdot s_{i,1}^{r\cdot} + \cdots + s_{i,\frac{N}{2}}^{l\cdot}\cdot s_{i,\frac{N}{2}}^{r\cdot}\right\} \in \mathbb{R}^{d_{p_3}\times\frac{N}{2}} \end{cases} \tag{6}$$

where $d_{p_1} = d_{p_2} = d_l$ and $d_{p_3} = 1$.[1]

To further capture the higher level discrepancy discriminative features, we utilize another RNN module that performs on the obtained differential asymmetric features $\{\hat{\mathbf{s}}_i^h\}$ and $\{\hat{\mathbf{s}}_i^v\}$ from the horizontal and vertical streams. Here, we can use the RNN module to extract the higher level features because the dimensions of the paired electrodes in the deep features $\hat{\mathbf{S}}_t^h$ and $\hat{\mathbf{S}}_t^v$ are same and thus can be treated as virtual sequence. Formally, the operations on them can be written as

$$\tilde{\mathbf{s}}_i^h = \sigma\left(\mathbf{U}^h\hat{\mathbf{s}}_i^h + \mathbf{V}^h\tilde{\mathbf{s}}_{i-1}^h + \mathbf{b}^h\right) \in \mathbb{R}^{d_g\times 1} \tag{7}$$

$$\tilde{\mathbf{s}}_i^v = \sigma\left(\mathbf{U}^v\hat{\mathbf{s}}_i^v + \mathbf{V}^v\tilde{\mathbf{s}}_{i-1}^v + \mathbf{b}^v\right) \in \mathbb{R}^{d_g\times 1} \tag{8}$$

where $\{\mathbf{U}^h \in \mathbb{R}^{d_g\times d_p}, \mathbf{V}^h \in \mathbb{R}^{d_g\times d_g}, \mathbf{b}^h \in \mathbb{R}^{d_g\times 1}\}$ and $\{\mathbf{U}^v \in \mathbb{R}^{d_g\times d_p}, \mathbf{V}^v \in \mathbb{R}^{d_g\times d_g}, \mathbf{b}^v \in \mathbb{R}^{d_g\times 1}\}$ are the learnable parameter matrices, and d_g is the dimension of the hidden unit of the high-level RNN module. Moreover, to automatically detect the salient information related to emotion among these paired differential features, two learnable projection matrices are applied to the higher level discrepancy discriminative features $\{\tilde{\mathbf{s}}_i^h\}$ and $\{\tilde{\mathbf{s}}_i^v\}$ obtained by (7) and (8). Denoting the projection matrices for the horizontal and vertical traversing directions by $\mathbf{W}^h = [w_{ik}^h]_{(N/2)\times K}$ and $\mathbf{W}^v = [w_{ik}^v]_{(N/2)\times K}$, the projection can be written as

$$\bar{\mathbf{s}}_k^h = \sigma\left(\sum_{i=1}^{N/2} w_{ik}^h\tilde{\mathbf{s}}_i^h + \hat{\mathbf{b}}^h\right) \in \mathbb{R}^{d_g\times 1},\ k = 1, 2, \ldots, K \tag{9}$$

$$\bar{\mathbf{s}}_k^v = \sigma\left(\sum_{i=1}^{N/2} w_{ik}^v\tilde{\mathbf{s}}_i^v + \hat{\mathbf{b}}^v\right) \in \mathbb{R}^{d_g\times 1},\ k = 1, 2, \ldots, K. \tag{10}$$

Finally, we use two learnable mapping matrices $\mathbf{G}^h \in \mathbb{R}^{d_o\times d_g}$ and $\mathbf{G}^v \in \mathbb{R}^{d_o\times d_g}$ to summarize the stimulus $\bar{\mathbf{S}}_t^h = \{\bar{\mathbf{s}}_k^h\} \in \mathbb{R}^{d_g\times K}$ and $\bar{\mathbf{S}}_t^v = \{\bar{\mathbf{s}}_k^v\} \in \mathbb{R}^{d_g\times K}$ from two directional streams, and then form the final feature representation, namely

$$\mathbf{S}_t^{hv} = \mathbf{G}^h\bar{\mathbf{S}}_t^h + \mathbf{G}^v\bar{\mathbf{S}}_t^v \in \mathbb{R}^{d_o\times K}. \tag{11}$$

Till now, for an input EEG sample $\mathbf{X}_t$, the output feature $\mathbf{S}_t^{hv}$ is obtained.

C. Discriminative Prediction and Domain Adversarial Strategy

As in most supervised models, we add a supervision term into the network by applying the softmax function to the output feature $\mathbf{S}_t^{hv} = \{\mathbf{s}_k^{hv}\}$, $(k = 1, \ldots, K)$ to predict the class label.

[1]Precisely, division operation models the differential information in terms of the relative ratio of magnitude; the (minus) inner product operation models such information in terms of (dis) similarity.

Let $\mathbf{o} = [(\mathbf{s}_1^{hv})^T, (\mathbf{s}_2^{hv})^T, \ldots, (\mathbf{s}_K^{hv})^T] \in \mathbb{R}^{1\times Kd_o}$ denote the output feature vector. It can be shown that

$$\mathbf{y} = \mathbf{oP} + \mathbf{b}^c = \{y_1, y_2, \ldots, y_C\} \in \mathbb{R}^{1\times C} \tag{12}$$

where $\mathbf{P} \in \mathbb{R}^{Kd_o\times C}$ and $\mathbf{b}^c \in \mathbb{R}^{1\times C}$ are the transform matrices, and C is the number of emotion classes.

Finally, the output vector of BiHDM is fed into the softmax layer for emotion classification, which can be written as

$$P(c|\mathbf{X}_t) = \exp(y_c)/\sum_{i=1}^{C}\exp(y_i) \tag{13}$$

where $P(c|\mathbf{X}_t)$ denotes the predicted probability that the input sample $\mathbf{X}_t$ belongs to the cth class. As a result, the label $\tilde{l}_t$ of sample $\mathbf{X}_t$ is predicted as

$$\tilde{l}_t = \arg\max_c P(c|\mathbf{X}_t). \tag{14}$$

Consequently, the loss function of the classifier can be expressed as

$$L_c\big(\mathbf{X}_t;\theta_f,\theta_c\big) = \sum_{t=1}^{M_1}\sum_{c=1}^{C} -\tau(l_t,c)\times \log P(c|\mathbf{X}_t) \tag{15}$$

$$\tau(l_t,c) = \begin{cases} 1, & \text{if } l_t = c \\ 0, & \text{otherwise.} \end{cases} \tag{16}$$

Here, θ_f and θ_c denote the learnable parameters of the feature extraction module and the classifier, while l_t and M_1 are the ground-truth label of sample $\mathbf{X}_t$ and the number of source (training) samples. By minimizing the above loss function, discriminative features could be extracted for emotion recognition.

Recall that we need to consider the potential data distribution shift for EEG emotional signal, especially in the case of subject-independent task where the source and target data come from different subjects. Here, we assume that the unlabeled target (testing) data are known in advance and to align the feature distributions between source and target domains, we further adopt the domain adversarial strategy by adding a discriminator into the network. It works cooperatively with the classifier to induce the feature extraction process to generate emotion discriminative but domain-invariant features.

Concretely, we predefine the source domain label set $D_S = \{0, 0, \ldots, 0\} \in \mathbb{Z}^{M_1\times 1}$ and the target domain label set $D_T = \{1, 1, \ldots, 1\} \in \mathbb{Z}^{M_2\times 1}$, where M_2 is the number of unlabeled target samples. Then through maximizing the loss function of the discriminator, which can be denoted as

$$L_d\Big(\mathbf{X}_t^S, \mathbf{X}_{t'}^T; \theta_f, \theta_d\Big) = -\sum_{t=1}^{M_1}\log P\Big(0|\mathbf{X}_t^S\Big) - \sum_{t'=1}^{M_2}\log P\big(1|\mathbf{X}_{t'}^T\big) \tag{17}$$

the feature extraction process expects to have the ability to generate the data representation to confuse the discriminator that aims to distinguish which domain the input comes from (i.e., the domain-invariant features). Here, $\mathbf{X}_t^S$ and $\mathbf{X}_{t'}^T$ denote the tth and t'th samples in the source and target data set, respectively, and θ_d represents the learnable parameter of discriminator.

D. Optimization of BiHDM

The overall optimization of BiHDM can be expressed as

$$\min L\big(\mathbf{X};\theta_f,\theta_c,\theta_d\big) = L_c\Big(\mathbf{X}^S;\theta_f,\theta_c\Big) - L_d\Big(\mathbf{X}^S,\mathbf{X}^T;\theta_f,\theta_d\Big) \tag{18}$$

where $L(\cdot)$ is the loss function of the overall model, and $\mathbf{X}$ denotes the entire data set that consists of the source data set $\mathbf{X}^S$ and target data set $\mathbf{X}^T$, i.e., $\mathbf{X} = [\mathbf{X}^S, \mathbf{X}^T] \in \mathbb{R}^{d\times N\times(M_1+M_2)}$.

This max–minimization loss function will force the parameters of the feature extraction module to generate emotion discriminative but domain-invariant data representation, which benefits EEG emotion recognition because of the potential data distribution shift for EEG emotional signal, especially in the case of subject-independent task where the source and target data come from different subjects.

Specifically, the maximization problem can be transferred to a minimization problem by using a gradient reversal layer (GRL) [21] before the discriminator as shown in Fig. 1, which can be optimized by using the stochastic gradient descent (SGD) algorithm [28] easily. GRL acts as an identity transform in the forward propagation but reverses the gradient sign while performing the backward-propagation operation. The overall optimization process follows the rules:

$$\theta_c \leftarrow \theta_c - \alpha\frac{\partial L_c}{\partial\theta_c}, \quad \theta_d \leftarrow \theta_d - \alpha\frac{\partial L_d}{\partial\theta_d} \tag{19}$$

$$\theta_f \leftarrow \theta_f - \alpha\left(\frac{\partial L_c}{\partial\theta_f} - \frac{\partial L_d}{\partial\theta_f}\right) \tag{20}$$

where α is the learning rate. In this way, we can iteratively train the classifier and the discriminator to update the parameters with the similar approach of standard deep learning methods by the chain rule.

IV. Experiments

A. Experimental Setting

To evaluate the proposed BiHDM model, in this section, we will conduct experiments on three public EEG emotional data sets. All the three data sets were collected when the participants sat in front of a monitor comfortably and watched emotional video clips. The EEG signals are recorded from 62 electrode channels using ESI NeuroScan[2] with a sampling rate of 1000 Hz. The locations of electrodes are on the basis of the international 10–20 system. Thus, in the experiment, we perform the pairwise operation on the 31 paired electrodes based on the symmetric locations on the left and right brain hemispheric scalps. The detailed information of these data sets is described as follows.

1) *SEED [12]:* The SEED data set contains 15 subjects, and each subject has three sessions. During the experiment, the participants watched three kinds of emotional film clips, i,e, *happy*, *neutral*, and *sad*, where each emotion has five film clips. Consequently, there are totally 15

[2]https://compumedicsneuroscan.com/

trials, and each trial has 185–238 samples for one session of each subject. Then there are totally about 3400 samples in one session.

2) *SEED-IV*[3] *[5]:* The SEED-IV data set also contains 15 subjects, and each subject has three sessions. But it includes four emotion types with the extra emotion *fear* compared with SEED, and each emotion has six film clips. Thus, there are totally 24 trials, and each trial has 12–64 samples for one session of each subject. Then there are totally about 830 samples in one session.
3) *MPED*[3] *[27]:* The MPED data set contains 30 subjects and each subject has one session. It includes seven refined emotion types, i.e., *joy*, *funny*, *neutral*, *sad*, *fear*, *disgust*, and *anger*, and each emotion has four film clips. There are totally 28 trials, and each trial has 120 samples. There are totally 3360 samples in one subject.

To evaluate the proposed BiHDM model adequately, we design two kinds of experiments, including the subject-dependent and subject-independent ones. In the subject-dependent experiment, both source (training) and target (testing) data come from the same subject but different EEG trials; while in the subject-independent experiment, the source and target data come from different subjects. We use the released handcrafted features, i.e., the differential entropy (DE) in SEED and SEED-IV, and the short-time Fourier transform (STFT) in MPED, as the input to feed our model. Thus, the sizes $d \times N$ of the input sample $\mathbf{X}_t$ are 5×62, 5×62, and 1×62 for these three data sets, respectively.[4] Moreover, in the experiment, we, respectively, set the dimension d_l of each electrode's deep representation to 32; the parameters d_g and K of the global high-level feature to 32 and 6; and the dimension d_o of the output feature to 16. Specifically, we implemented BiHDM using TensorFlow[5] on one Nvidia 1080Ti GPU. The learning rate, momentum, and weight decay rate are set as 0.003, 0.9, and 0.95, respectively. The network is trained using SGD with a batch size of 200. In addition, we adopt the subtraction as the pairwise operation of the BiHDM model, and discuss the other two types of operations in Section IV-C2.

B. Experimental Results for EEG Emotion Recognition

1) Subject-Dependent Experiment: In this experiment, we adopt the same protocols as [5], [12], and [27]. Namely, for SEED, we use the former nine trials of EEG data per session of each subject as source (training) domain data while using the remaining six trials per session as target (testing) domain data; for SEED-IV, we use the first sixteen trials per session of each subject as the training data, and the last eight trials containing all emotions (each emotion with two trials) as the testing data; for MPED, we use 21 trials of EEG data as training data and the rest seven trials consist of seven emotions as testing data for each subject. The mean accuracy (ACC) and standard deviation (STD) are used as the evaluation criteria for all the subjects in the data set.

TABLE I
CLASSIFICATION PERFORMANCE FOR SUBJECT-DEPENDENT EEG EMOTION RECOGNITION ON SEED, SEED-IV, AND MPED DATA SETS

Method	ACC / STD (%)		
	SEED	SEED-IV	MPED
SVM [29]	83.99/09.72	56.61/20.05*	32.39/09.53*
RF [30]	78.46/11.77	50.97/16.22*	23.83/06.82*
CCA [31]	77.63/13.21	54.47/18.48*	29.08/07.96*
GSCCA [10]	82.96/09.95	69.08/16.66*	36.78/07.76*
DBN [12]	86.08/08.34	66.77/07.38*	35.07/11.25*
GRSLR [24]	87.39/08.64	69.32/19.57*	34.58/08.41*
GCNN [32]	87.40/09.20	68.34/15.42*	33.26/06.44*
DGCNN [26]	90.40/08.49	69.88/16.29*	32.37/06.08*
DANN [21]	91.36/08.30	63.07/12.66*	35.04/06.52*
BiDANN [33]	92.38/07.04	70.29/12.63*	37.71/06.04*
EmotionMeter [5]	–	70.59/17.01	–
A-LSTM [27]	88.61/10.16*	69.50/15.65*	38.99/07.53*
BiHDM	**93.12/06.06**	**74.35/14.09**	**40.34/07.59**

∗ indicates the experiment results obtained by our own implementation.
– indicates the experiment results are not reported on that dataset.

To validate the classification superiority of BiHDM, we also conduct the same experiments using another 12 methods, including linear support vector machine (SVM) [29], random forest (RF) [30], canonical correlation analysis (CCA) [31], GSCCA [10], DBN [12], GRSLR [24], graph convolutional neural network (GCNN) [32], DGCNN [26], DANNs [21], bi-hemisphere DANN (BiDANN) [33], EmotionMeter [5], and A-LSTM [27]. All the methods are the representative ones in the previous studies of emotion recognition. We directly quote (or reproduce) their results from the literature to ensure a convincing comparison with the proposed method. The results are summarized in Table I.

From Table I, we can see that the proposed BiHDM model outperforms all the compared methods on all the three public EEG emotional data sets, which verifies the effectiveness of BiHDM. Especially, for the result on SEED-IV, the proposed method improves over the state-of-the-art method EmotionMeter by 4%. Besides, we can see that the compared method BiDANN, which also considers the difference between the left and right hemispheric data, achieves the overall closest performance to the proposed BiHDM. The main difference between BiDANN and BiHDM is that the former considers the difference of data distribution between two hemispheres and adopts two hemispheric feature extractors to separately obtain the data representation but not directly captures the discrepancy information. In contrast, the latter (i.e., the proposed BiHDM) focuses on constructing a model to learn the discrepancy relation between two hemispheres and these differential components are beneficial for emotion recognition. Meanwhile, both the results of BiHDM and BiDANN indicate the importance of considering the difference between the left and right cerebral hemispheric data for EEG emotion recognition.

[3]Note that both SEED-IV and MPED are multimodal data sets. MPED consists of 30 subjects' EEG data, among which 23 subjects contain multimodal data. In this experiment, we only use the EEG modal data.

[4]Note that the proposed BiHDM model is trained on all the electrodes, including that in the middle to avoid losing any information of the EEG data. Concretely, there are eight electrodes in the middle for the three data sets used in the experiment. Thus, we concatenate the four forehead electrodes with the left hemispheric EEG data, while the other four electrodes on the backside of the head as the right hemispheric EEG data.

[5]https://www.tensorflow.org/

TABLE II
t-TEST STATISTICAL ANALYSIS BETWEEN BIHDM AND THE STATE-OF-THE-ART METHOD BIDANN AT THE SIGNIFICANCE LEVEL OF 0.05. WHEN THE IMPROVEMENT OF BIHDM OVER THE METHOD IS STATISTICALLY SIGNIFICANT, THE RESULT WILL BE UNDERLINED

Method	Experiment	p-value		
		SEED	SEED-IV	MPED
BiHDM vs. BiDANN	Subject-dependent	0.0580	<u>0.0344</u>	<u>0.0488</u>
	Subject-independent	<u>0.0451</u>	<u>0.0188</u>	<u>0.0091</u>

To test if the proposed BiHDM is statistically significantly better than the closest performance method BiDANN, we perform the paired *t*-test statistical analysis between them at a significant level of 0.05. When the improvement of BiHDM over the method is statistically significant, the results will be underlined in the table. The first row of Table II shows the *t*-test statistical analysis results, from which we can see BiHDM is indeed significantly better than the baseline method on two out of three data sets. For the data set SEED, the *p*-value is also close to 0.05.

Besides, although the representative methods DANN and BiDANN in Table I have used the unlabeled testing data to enhance their performance, some compared methods only use the labeled training data to learn the model. To have a fair comparison with them, we follow their setting by removing the discriminator from the proposed BiHDM and only using the labeled training data to conduct the same experiments. The accuracies of the proposed BiHDM become 91.07%, 72.22%, and 38.55% on SEED, SEED-IV, and MPED data sets, which are still the state-of-the-art performance on SEED and SEED-IV data sets and very close to the best performance on the MPED data set compared with the methods that trained without the unlabeled test data. This indicates our differential features are indeed more discriminative.

2) Subject-Independent Experiment: In this experiment, we adopt the leave-one-subject-out (LOSO) cross-validation strategy [34] to evaluate the proposed BiHDM model. The LOSO strategy uses the EEG signals of one subject as testing data and the rest subjects' EEG signals as training data. This procedure is repeated such that the EEG signals of each subject will be used as testing data once. Again, the mean accuracy (ACC) and STD are used as the evaluation criteria.

Recall that the distribution gap in the subject-independent task is much larger than that in the subject-dependent one. In this case, domain adaptation methods shall be properly employed in order to achieve promising performance. Therefore, in the experiment on the subject-independent task, we include many domain adaptation methods in the comparison. By doing so, we can effectively validate the state-of-the-art performance of our method. We compare our method with another 12 methods, including Kullback–Leibler importance estimation procedure (KLIEP) [35], unconstrained least-squares importance fitting (ULSIF) [36], selective transfer machine (STM) [37], linear SVM, transfer component analysis (TCA) [38], subspace alignment (SA) [39], geodesic flow kernel (GFK) [40], DANN, DGCNN, deep adaptation network (DAN) [41], BiDANN, and A-LSTM, to conduct the same experiments. All these methods are the representative ones in the previous studies of emotion recognition, and most of them adopt the domain adaptation technique to train the model with the labeled training data and unlabeled testing data. The results are shown in Table III.[6]

TABLE III
CLASSIFICATION PERFORMANCE FOR SUBJECT-INDEPENDENT EEG EMOTION RECOGNITION ON SEED, SEED-IV, AND MPED DATA SETS

Method	ACC / STD (%)		
	SEED	SEED-IV	MPED
KLIEP [35]	45.71/17.76	31.46/09.20*	18.92/04.54*
ULSIF [36]	51.18/13.57	32.99/11.05*	19.63/03.81*
STM [37]	51.23/14.82	39.39/12.40*	20.89/03.62*
SVM [29]	56.73/16.29	37.99/12.52*	19.66/03.96*
TCA [38]	63.64/14.88	56.56/13.77*	19.50/03.61*
SA [39]	69.00/10.89	64.44/09.46*	20.74/04.17*
GFK [40]	71.31/14.09	64.38/11.41*	20.27/04.34*
A-LSTM [27]	72.18/10.85*	55.03/09.28*	24.06/04.58*
DANN [21]	75.08/11.18	47.59/10.01*	22.36/04.37*
DGCNN [26]	79.95/09.02	52.82/09.23*	25.12/04.20*
DAN [41]	83.81/08.56	58.87/08.13	–
BiDANN [33]	83.28/09.60	65.59/10.39*	25.86/04.92*
BiHDM	**85.40/07.53**	**69.03/08.66**	**28.27/04.99**

∗ indicates the experiment results obtained by our own implementation.
– indicates the experiment results are not reported on that dataset.

From Table III, it can be clearly seen that the proposed BiHDM method achieves the best performance on all the three public data sets, which verifies the effectiveness of BiHDM in dealing with subject-independent EEG emotion recognition. For the three data sets, the improvements on accuracy are 2.2%, 3.5%, and 2.4%, respectively, when compared with the state-of-the-art method BiDANN. Furthermore, we perform the paired *t*-test between BiHDM and BiDANN at the significant level of 0.05. The second row of Table II shows the *t*-test statistical analysis results, from which we can see BiHDM is significantly better than BiDANN on all the three data sets.

Besides, to further verify that the asymmetry information obtained by BiHDM plays a dominant role in the performance improvement rather than the domain adaptation strategy, we conduct additional experiments on SEED, SEED-IV, and MPED data sets by ablating the discriminator of BiHDM, and obtain 81.55%, 67.47%, and 27.43% in accuracy, respectively. These results are clearly superior to most of the compared methods, which shows the extracted discrepancy feature indeed is helpful for EEG emotion recognition. Besides, we can also observe that, with domain discriminator, the performance can be further improved, which shows the effectiveness of considering the domain gap in EEG emotion recognition tasks.

[6]Note that the subspace-based methods, such as TCA, SA, and GFK, are problematic to handle a large amount of EEG data due to the computer memory limitation and computational issue. Therefore, to compare with them we have to randomly select 3000 EEG feature samples from the training data set to train these methods.

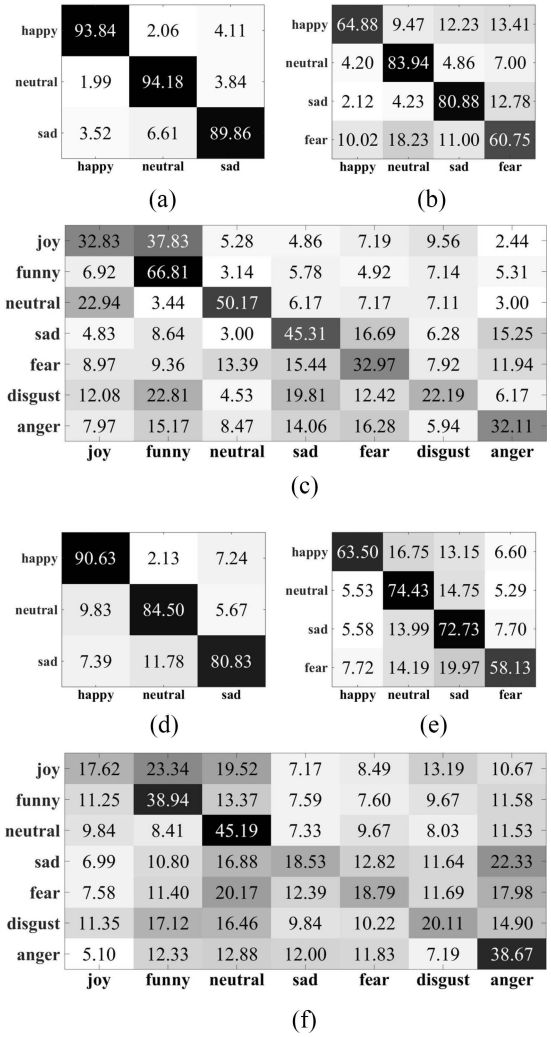

Fig. 2. Confusion matrices of the proposed method BiHDM on three data sets. (a) and (d) SEED. (b) and (e) SEED-IV. (c) and (f) MPED.

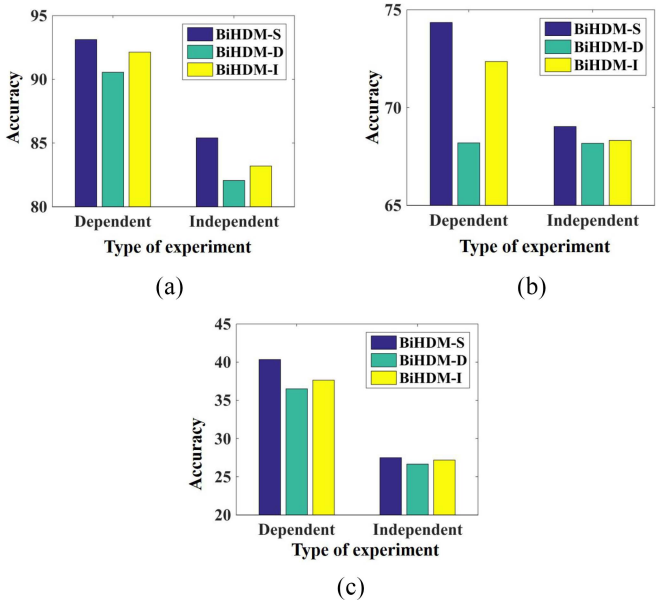

Fig. 3. Experimental results of BiHDM-S, BiHDM-D, and BiHDM-I models on three data sets. In each figure, the marks "Dependent" and "Independent" on horizontal axis indicate the subject-dependent and independent experiments, respectively. (a) SEED. (b) SEED-IV. (c) MPED.

C. Discussion

1) Confusion of Different Emotions Based on the BiHDM Model: To better understand the confusions of BiHDM in recognizing different emotions, we depict the confusion matrices of the above two experiments in Fig. 2. We have two observations in the following.

1) From Fig. 2(a) and (d) corresponding to the SEED data set, we can see that the emotions *happy* and *neutral* are much easier to be recognized than *sad*. Furthermore, in Fig. 2(d), the recognition rates of emotions *neutral* and *sad* decrease about 10% and 9% while the emotion *happy* only decreases 3% compared with the results in Fig. 2(a). We can observe the similar case from the two confusion matrices of the SEED-IV data set from Fig. 2(b) and (e). This shows that the emotion *happy* associates with more similar brain reflection over different people than *neutral* and *sad*.
2) MPED, which consists of seven emotion types, is much more complicated than the other two data sets. From the subject-dependent result in Fig. 2(c), we can find that the emotions *funny*, *neutral*, and *sad* are much easier to be recognized than the other four emotions. However, comparing it with the subject-independent confusion matrix in Fig. 2(f), we can see that the recognition rate of *sad* decreases significantly, which is same as the case observed in the above [i.e., point 1)]. It is possibly because the pattern of emotion *sad* varies considerably from one subject to another.

2) Performance Based on Different Pairwise Operations: In this section, we investigate the performance of using different pairwise operations in BiHDM, as shown in (6). Here, we denote the subtraction, division, and inner product variants as BiHDM-S, BiHDM-D, and BiHDM-I, respectively. The results are shown in Fig. 3. As seen, the subtraction operation achieves the best performance among the three pairwise operations. We attribute this to the fact that the subtraction operation directly measures the discrepancy between two hemispheres, whereas the other two operations describe the difference in a less straightforward manner. Meanwhile, both BiHDM-I and BiHDM-D still achieve comparable performance compared with the other methods shown in Tables I and III, which can show the effectiveness of considering the differential information between two cerebral hemispheres. We will explore more pairwise operations, such as nonlinear kernel functions in the future work.

Moreover, to better understand the three variants of BiHDM in recognizing different emotions, we depict the confusion matrices of BiHDM-D and BiHDM-I in Figs. 4 and 5, respectively. Overall, there are some similar observations with BiHDM-S in Fig. 2 of Section IV-C1. Nevertheless, there are some differences among them.

1) From Figs. 2(a), 4(a), and 5(a) corresponding to the SEED data set, we can see that BiHDM-S can

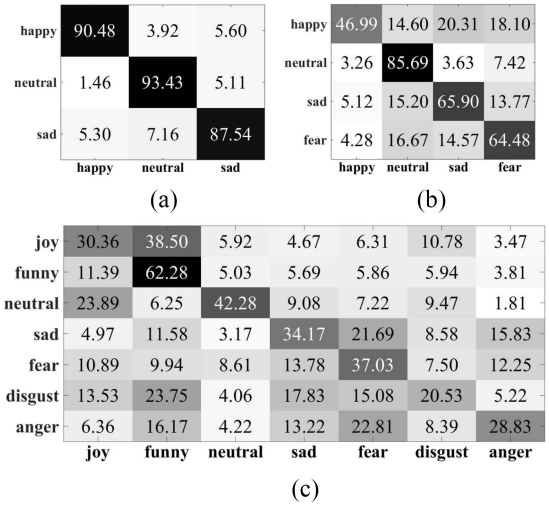

Fig. 4. Confusion matrices based on subject-dependent experiments of BiHDM-D on three data sets. (a) SEED. (b) SEED-IV. (c) MPED.

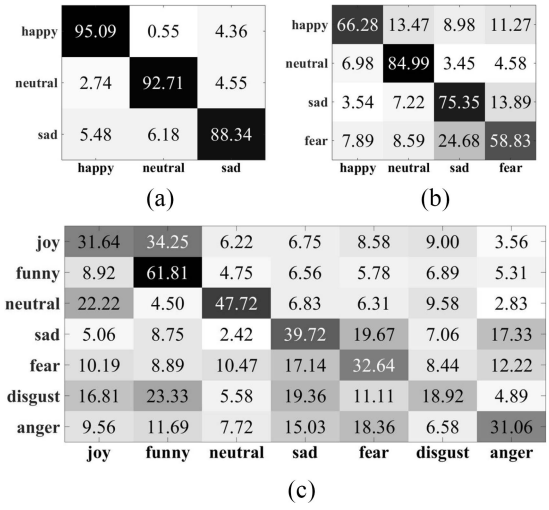

Fig. 5. Confusion matrices based on subject-dependent experiments of BiHDM-I on three data sets. (a) SEED. (b) SEED-IV. (c) MPED.

outperform BiHDM-D and BiHDM-I mainly due to the better recognition rates for emotions *neutral* and *sad*.

2) Besides, from the results on SEED-IV data set as shown in Figs. 2(b), 4(b), and 5(b), it is clear to see that BiHDM-D fails in recognizing the emotions *happy* and *sad* (the decrease is above 15% compared with BiHDM-S), meanwhile BiHDM-I is not good at recognizing emotion *sad* (the decrease is about 5% compared with BiHDM-S).
3) For the MPED data set, BiHDM-S can achieve the best performance in recognizing all types of emotions except *fear*.

This provides a detailed explanation about why BiHDM-S outperforms BiHDM-D and BiHDM-I.

The above experiments have verified the excellent classification performance of BiHDM. The major reason lies at that the pairwise operations in BiHDM effectively computes the discrepancy information between two hemispheres by considering the specific emotion-related property of EEG

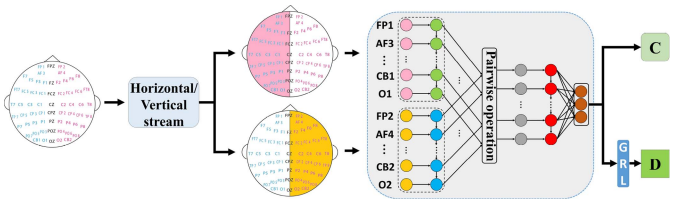

Fig. 6. Framework of BiHDM-h/v.

emotional signals. Besides, we note that in one previous study [42], Zheng *et al.* also found that the brain processing related to positive, neutral, and negative emotions have asymmetrical characteristics. But in the experiment section, they showed that the proposed original channel-based features achieved comparable or even better results than the asymmetry features in DEAP and SEED data sets, respectively. The difference between this article and ours is that the overall structure in BiHDM is designed for learning the deep asymmetry information. To verify that this asymmetry information obtained by BiHDM is indeed more helpful for emotion recognition than the original channel-based features, we conduct additional experiments for subject-dependent EEG emotion recognition on SEED, SEED-IV, and MPED data sets by replacing the pairwise operation with a direct concatenation of the paired electrodes' deep representations, and obtain 90.52%, 72.68%, and 37.89% in accuracy, respectively. The concatenation operation is clearly inferior to the proposed subtraction operation (93.12%, 74.35%, and 40.34%). This shows that using the pairwise operation to explicitly extract the discrepancy indeed helps EEG emotion recognition.

3) Effect of Two Directional RNNs to Extract Spatial Information: In BiHDM, the horizontal and vertical RNNs are adopted to model the structural relation between the electrodes. To evaluate the effect of this spatial information extraction for emotion recognition, we modified the framework of BiHDM with a single directional RNN shown in Fig. 6, denoted by BiHDM-h and BiHDM-v, respectively, to conduct the same experiments. The results are summarized in Table IV, from which we can see that the predefined strategy of traversing the spatial region with horizontal and vertical RNNs achieves much better performance than the single directional RNN.

To investigate which emotion can be better recognized with the spatial information extraction, we depict the confusion matrices of BiHDM-h and BiHDM-v in Fig. 7. Compared with the confusion matrices of BiHDM shown in Fig. 2, we can see that, with the structural relation between the electrodes, BiHDM achieves better performance in recognizing all types of emotions than BiHDM-h and BiHDM-v. Especially, for the emotion *sad*, the structural information helps the model greatly. Concretely, for the three data sets, the improvements on accuracy are 10%, 15%, and 9% compared with BiHDM-h, and 10%, 11%, and 7% compared with BiHDM-v, respectively. This shows that the proposed spatial feature learning method is helpful to extract the discriminative information and that the spatial relation between different electrodes can indeed exert a positive impact to EEG emotion recognition.

TABLE IV
CLASSIFICATION PERFORMANCE OF DIFFERENT SPATIAL FEATURE EXTRACTION METHODS FOR EEG EMOTION RECOGNITION ON SEED, SEED-IV, AND MPED DATA SETS. HERE, BIHDM-H AND BIHDM-V DENOTE THE MODIFIED BIHDM MODELS WITH ONLY HORIZONTAL AND VERTICAL STREAMS RESPECTIVELY, NAMELY, THE UPPER AND BOTTOM HALF PARTS IN FIG. 1. (a) SUBJECT-DEPENDENT EXPERIMENTAL RESULTS. (b) SUBJECT-INDEPENDENT EXPERIMENTAL RESULTS

(a)

Electrode area	ACC / STD (%)		
	SEED	SEED-IV	MPED
BiHDM-h	87.47/09.17	62.06/15.01	36.24/08.41
BiHDM-v	86.75/07.09	65.57/15.43	36.69/08.20
BiHDM	**93.12/06.06**	**74.35/14.09**	**40.34/07.59**

(b)

Electrode area	ACC / STD (%)		
	SEED	SEED-IV	MPED
BiHDM-h	82.38/09.33	66.80/08.22	28.05/04.98
BiHDM-v	81.03/10.28	66.96/08.28	27.86/05.06
BiHDM	**85.40/07.53**	**69.03/08.66**	**28.27/04.99**

4) Activity of EEG Electrodes: In the previous literature, neuroscience researchers have investigated the asymmetry between hemispheres of the brain that is related to emotions [1], [13], [14]. For example, a relative left frontal activation is associated with positive emotions, while a greater right frontal activation associated with negative emotions. Thus, the asymmetry on the frontal brain areas may mainly reflect the differential information that is helpful for emotion recognition [43]–[46]. Meanwhile, some researches have revealed that the temporal asymmetry is present for emotion recognition [47]. To clearly illustrate the contribution of the differential information from various brain areas for emotion expression, we depict the electrode activity maps in Fig. 8. The contribution is evaluated by computing the 2-norm of each column of the asymmetric differential features $\hat{\mathbf{S}}_t^h$ and $\hat{\mathbf{S}}_t^v$ in (4) and (5) for all the testing data and mapping these values into the corresponding electrodes. Note that the two electrodes in a pair share the same value because it is computed by the pairwise operation. From Fig. 8, we can see that the frontal EEG asymmetry plays a more important role in emotion recognition for all the three data sets. Moreover, from Fig. 8(c), we can clearly observe that the temporal lobe asymmetry also makes an important contribution as the frontal asymmetry, which reveals the significance of these two brain areas in discriminating more types of emotion. These observations are consistent with the cognition observation in biological psychology [48], [49], namely, the frontal and temporal lobes are the main areas of the brain correlated with emotional activity [8].

Furthermore, to explore where the differential information comes from in terms of the emotion expressed, we separately depict the electrode activity maps corresponding to each emotion in Fig. 9. Although it looks quite similar with Fig. 8, i.e., the asymmetry on frontal and temporal lobes makes more contribution to discriminating different emotions, we can observe some subtle distinctions from these maps.

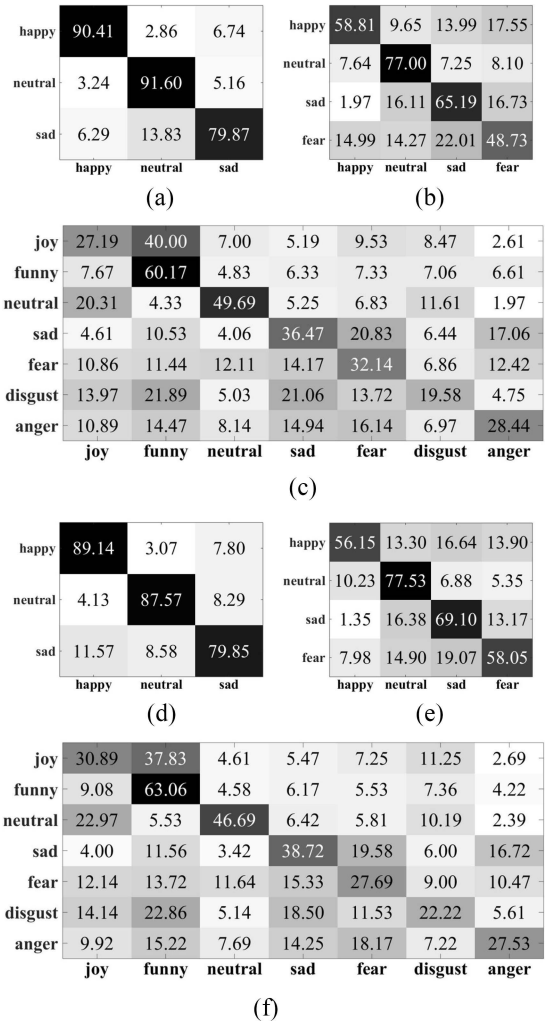

Fig. 7. Confusion matrices of different spatial feature extraction methods of BiHDM for subject-dependent experiments on three data sets. Here, BiHDM-h and BiHDM-v denote the modified BiHDM model with only horizontal and vertical streams, respectively, namely, the upper and bottom half parts in Fig. 1. (a) and (d) SEED. (b) and (e) SEED-IV. (c) and (f) MPED.

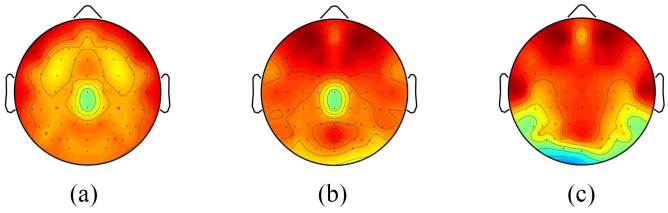

Fig. 8. EEG electrode activity maps of the subject-dependent experiments. Darker red denotes more significant contribution. Note that these maps are symmetric because it shows the value computed by the pairwise operation applied to paired electrodes. (a) SEED. (b) SEED-IV. (c) MPED.

1) For the positive emotions (*happy* in SEED and SEED-IV and *joy* and *funny* in MPED), we can see that the asymmetry on temporal lobe has the same contribution as (or even more than) the frontal lobe.
2) On the contrary, for the neutral emotion [Fig. 9(b), (e), and (j)], the asymmetry on frontal lobe contributes more than temporal lobe.

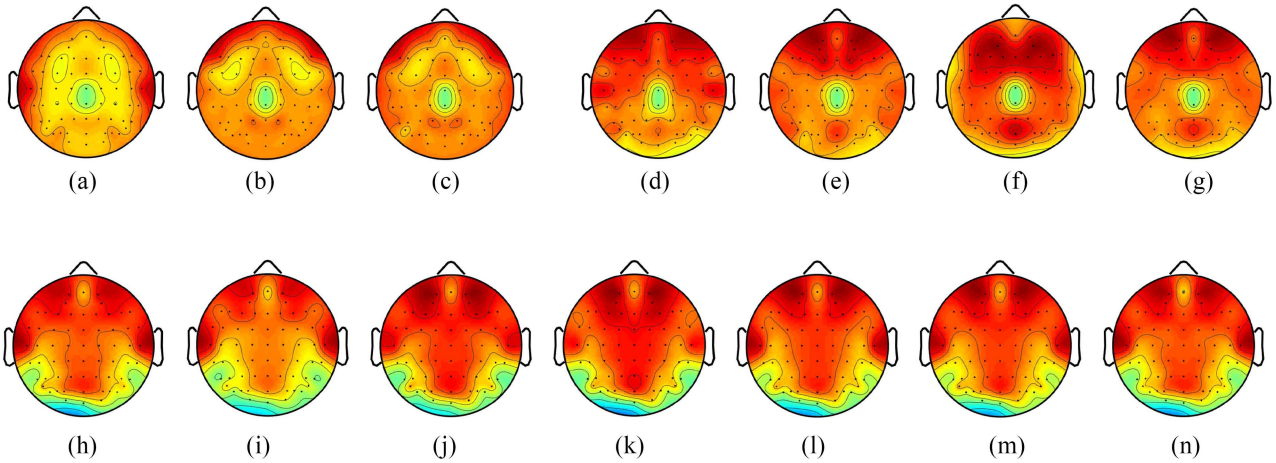

Fig. 9. EEG electrode activity maps in terms of different emotions based on the results of the proposed BiHDM model in subject-dependent experiments. Darker red denotes more significant contribution. (a)–(c), (d)–(g), and (h)–(n) are the results on SEED, SEED-IV, and MPED data sets, respectively. Note that these maps are symmetric because the values in each map are computed by the pairwise operation and applied to the paired electrodes.

3) For the *sad* emotion [Fig. 9(c), (f), and (k)], the asymmetry on frontal lobe basically dominates this emotion expression. Meanwhile, we can find that there is a broad activation area close to the frontal-central lobe, especially in SEED-IV and MPED which contain more types of emotions than SEED.
4) For the *fear* emotion, the asymmetry on frontal lobe dominates the emotion expression on the SEED-IV data set [Fig. 9(g)]. However, on the MPED data set, which includes more negative emotions (*anger* and *disgust*), the temporal lobe has the same contribution with the frontal lobe [Fig. 9(l)].

In summary, we can observe from these results of BiHDM that, for EEG emotional signal, there are two important brain areas, i.e., frontal and temporal lobes, which generally play important roles in the emotion expression. These observations can help us to select important electrodes for EEG emotion recognition in real-world applications, as demonstrated in the next section.

5) Performance Based on Less Electrodes: For the emotion recognition system in real-world applications, fewer electrodes will be preferred considering the feasibility and comfort. Thus, in this section, we investigate how the performance of the proposed BiHDM model varies with relatively small numbers of electrodes. Motivated by the results from Figs. 8 and 9, we select the paired electrodes on the two important brain areas referring to the locations of frontal and temporal lobes, denoted by *Frontal (6)*, *Frontal (10)*, *Temporal (6)*, and *Temporal (9)*,[7] where *Frontal (6)* and *Temporal (6)*, respectively, include the electrodes on the areas of frontal and temporal lobes while *Frontal (10)* and *Temporal (9)* further include some electrodes that are close to these two important brain areas. The experimental results are shown in Table V.

[7]Concretely, *Frontal (6)* includes the paired electrodes of FP1-Fp2, AF3-AF4, F7-F8, F5-F6, F3-F4, and F1-F2; *Frontal (10)* includes the paired electrodes of *Frontal (6)* and FT7-FT8, FC5-FC6, FC3-FC4, and FC1-FC2; *Temporal (6)* includes the paired electrodes of FT7-FT8, FC5-FC6, T7-T8, C5-C6, TP7-TP8, and CP5-CP6; *Temporal (9)* includes the paired electrodes of *Temporal (6)* and FC3-FC4, C3-C4, and CP3-CP4.

TABLE V
CLASSIFICATION PERFORMANCE-BASED ONLY ON THE FRONTAL AND TEMPORAL LOBE EEG DATA FOR SUBJECT-DEPENDENT AND SUBJECT-INDEPENDENT EEG EMOTION RECOGNITION ON SEED, SEED-IV, AND MPED DATA SETS. (a) SUBJECT-DEPENDENT EXPERIMENTAL RESULTS. (b) SUBJECT-INDEPENDENT EXPERIMENTAL RESULTS

(a)

Electrode area	**ACC / STD (%)**		
	SEED	SEED-IV	MPED
Frontal (6)	80.15/09.86	57.93/13.88	29.02/05.68
Frontal (10)	84.49/08.83	63.02/16.95	32.37/06.79
Temporal (6)	88.16/08.03	64.88/15.76	**33.61/07.19**
Temporal (9)	**90.16/07.44**	**65.19/16.03**	33.13/07.06
All (31)	**93.12/06.06**	**74.35/14.09**	**40.34/07.59**

(b)

Electrode area	**ACC / STD (%)**		
	SEED	SEED-IV	MPED
Frontal (6)	74.33/08.70	67.28/08.19	23.54/02.73
Frontal (10)	80.28/09.94	**68.16/07.85**	25.44/04.95
Temporal (6)	**85.04/07.13**	65.07/08.74	26.07/04.32
Temporal (9)	84.09/07.78	66.92/08.74	**26.43/04.55**
All (31)	**85.40/07.53**	**69.03/08.66**	**28.27/04.99**

We can have two observations from this table.

1) The obtained recognition results based on fewer electrodes could be comparable with that based on all the 31 paired electrodes, especially on the SEED data set. This also verifies that the frontal and temporal lobes' asymmetry indeed contributes more to the EEG emotion recognition than other brain areas, which agrees with the observation of Figs. 8 and 9. It is, therefore, possible to use fewer electrodes in EEG emotion recognition systems.
2) Comparing these two important brain regions, we can see the results based on temporal lobe electrodes outperform that based on the frontal lobe. It seems that the temporal lobe associates more with emotion expression than the frontal lobe for EEG emotion recognition,

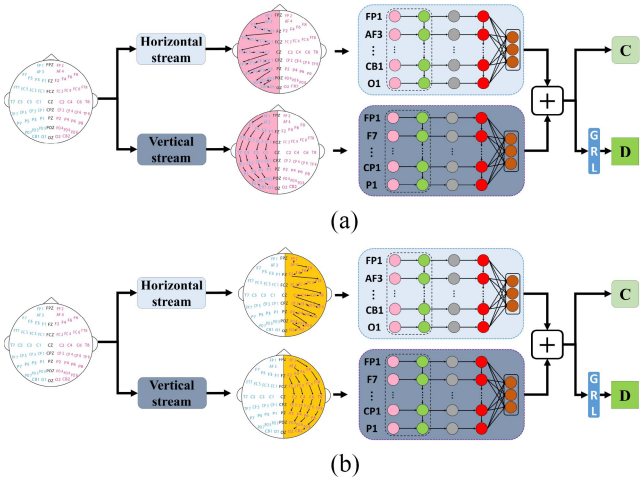

Fig. 10. Framework of (a) BiHDM-left and (b) BiHDM-right.

TABLE VI
CLASSIFICATION PERFORMANCE BASED ON SINGLE HEMISPHERIC EEG DATA FOR EEG EMOTION RECOGNITION ON SEED, SEED-IV, AND MPED DATA SETS. (a) SUBJECT-DEPENDENT EXPERIMENTAL RESULTS. (b) SUBJECT-INDEPENDENT EXPERIMENTAL RESULTS

(a)

Hemisphere	ACC / STD (%)		
	SEED	SEED-IV	MPED
BiHDM-left	**86.63/08.88**	**64.48/15.34**	**35.92/07.26**
BiHDM-right	86.39/07.54	60.11/13.53	33.08/08.30
BiHDM-overall	**93.12/06.06**	**74.35/14.09**	**40.34/07.59**

(b)

Hemisphere	ACC / STD (%)		
	SEED	SEED-IV	MPED
BiHDM-left	**78.88/09.01**	**64.93/07.96**	26.32/03.85
BiHDM-right	76.34/10.51	62.60/07.98	**27.41/05.32**
BiHDM-overall	**85.40/07.53**	**69.03/08.66**	**28.27/04.99**

especially on SEED and MPED data sets, which is consistent with the observations of [5] and [12].

6) Performance Based on Single Hemispheric EEG Data: From the above discussion, we can see the discrepancy information between the left and right hemispheres indeed contributes to the EEG emotion recognition task. Besides, it will be interesting to investigate which hemisphere is more tightly associated with emotion recognition. Therefore, in this section, we conduct the same experiments by separately feeding our modified BiHDM with the left and right hemispheric data (denoted by BiHDM-left and BiHDM-right shown in Fig. 10). The obtained results are shown in Table VI, from which we can see the left hemisphere is superior to the right for EEG emotion recognition. However, comparing it with the results in Table V, we can observe that those results are comparable or even better although the input data in Table VI uses more electrodes. This is opposite to the general knowledge that more electrodes should provide more information. We attribute this to the fact that the discrepancy information even obtained by a smaller number of electrodes could contain enough discrimination for emotion recognition, which verifies the effectiveness of discrepancy information from another aspect.

Hereto, we have evaluated the performance of the proposed BiHDM in subject-dependent and subject-independent experiments, investigated the important brain areas in emotion expression, and explored to use less electrodes to achieve comparable results. These experimental results jointly demonstrate the effectiveness and advantage of the proposed BiHDM model in solving the EEG emotion recognition problem.

V. CONCLUSION

In this article, we propose, a novel BiHDM for EEG emotion recognition, which is inspired by the neuroscience findings about the difference between the left and right brain hemispheres to the emotion expression. The proposed framework is easy to implement and the extensive experiments on three public EEG emotion data sets demonstrated that the proposed BiHDM method achieves the state-of-the-art performance. The better recognition performance of BiHDM mostly attributes to the fact that it can not only make use of the advantages of adversarial domain adaptation to improve the EEG recognition performance but also is able to make use of the differential information of two hemispheres in the perception of different emotions. Based on BiHDM, we also investigate the contribution of differential information from various brain areas for emotion expression, exploit the possibility of using less electrodes from important brain areas in practical EEG emotion recognition systems, and explore the classification performance based on a single hemispheric EEG data. In future work, we will further investigate more left and right hemispheric differential operations to explore the potential efficacy of cerebral hemisphere asymmetry in EEG emotion recognition.

REFERENCES

[1] S. J. Dimond, L. Farrington, and P. Johnson, "Differing emotional response from right and left hemispheres," *Nature*, vol. 261, no. 5562, p. 690, 1976.
[2] R. W. Picard, *Affective Computing*. Cambridge, MA, USA: MIT Press, 2000.
[3] R. Cowie *et al.*, "Emotion recognition in human–computer interaction," *IEEE Signal Process. Mag.*, vol. 18, no. 1, pp. 32–80, Jan. 2001.
[4] Y.-P. Lin *et al.*, "EEG-based emotion recognition in music listening," *IEEE Trans. Biomed. Eng.*, vol. 57, no. 7, pp. 1798–1806, May 2010.
[5] W.-L. Zheng, W. Liu, Y. Lu, B.-L. Lu, and A. Cichocki, "EmotionMeter: A multimodal framework for recognizing human emotions," *IEEE Trans. Cybern.*, vol. 49, no. 3, pp. 1110–1122, Mar. 2019.
[6] J. C. Britton, K. L. Phan, S. F. Taylor, R. C. Welsh, K. C. Berridge, and I. Liberzon, "Neural correlates of social and nonsocial emotions: An fMRI study," *Neuroimage*, vol. 31, no. 1, pp. 397–409, 2006.
[7] R. Jenke, A. Peer, and M. Buss, "Feature extraction and selection for emotion recognition from EEG," *IEEE Trans. Affect. Comput.*, vol. 5, no. 3, pp. 327–339, Jul.–Sep. 2014.
[8] S. M. Alarcão and M. J. Fonseca, "Emotions recognition using EEG signals: A survey," *IEEE Trans. Affect. Comput.*, vol. 10, no. 3, pp. 374–393, Jul.–Sep. 2019.
[9] B. García-Martínez, A. Martinez-Rodrigo, R. Alcaraz, and A. Fernández-Caballero, "A review on nonlinear methods using electroencephalographic recordings for emotion recognition," *IEEE Trans. Affect. Comput.*, early access, Jan. 1, 2019, doi: 10.1109/TAFFC.2018.2890636.

[10] W. Zheng, "Multichannel EEG-based emotion recognition via group sparse canonical correlation analysis," *IEEE Trans. Cogn. Develop. Syst.*, vol. 9, no. 3, pp. 281–290, Sep. 2017.
[11] P. Li *et al.*, "EEG based emotion recognition by combining functional connectivity network and local activations," *IEEE Trans. Biomed. Eng.*, vol. 66, no. 10, pp. 2869–2881, Oct. 2019.
[12] W.-L. Zheng and B.-L. Lu, "Investigating critical frequency bands and channels for EEG-based emotion recognition with deep neural networks," *IEEE Trans. Auton. Mental Develop.*, vol. 7, no. 3, pp. 162–175, Sep. 2015.
[13] R. J. Davidson, P. Ekman, C. D. Saron, J. A. Senulis, and W. V. Friesen, "Approach-withdrawal and cerebral asymmetry: Emotional expression and brain physiology: I," *J. Pers. Soc. Psychol.*, vol. 58, no. 2, p. 330, 1990.
[14] J. D. Herrington *et al.*, "Localization of asymmetric brain function in emotion and depression," *Psychophysiology*, vol. 47, no. 3, pp. 442–454, 2010.
[15] G. E. Schwartz, R. J. Davidson, and F. Maer, "Right hemisphere lateralization for emotion in the human brain: Interactions with cognition," *Science*, vol. 190, no. 4211, pp. 286–288, 1975.
[16] T. D. Wager, K. L. Phan, I. Liberzon, and S. F. Taylor, "Valence, gender, and lateralization of functional brain anatomy in emotion: a meta-analysis of findings from neuroimaging," *Neuroimage*, vol. 19, no. 3, pp. 513–531, 2003.
[17] E. Y. Costanzo *et al.*, "Hemispheric specialization in affective responses, cerebral dominance for language, and handedness: Lateralization of emotion, language, and dexterity," *Behav. Brain Res.*, vol. 288, pp. 11–19, Apr. 2015.
[18] F. Schroff, D. Kalenichenko, and J. Philbin, "FaceNet: A unified embedding for face recognition and clustering," in *Proc. IEEE Conf. Comput. Vis. Pattern Recognit.*, 2015, pp. 815–823.
[19] J. Schmidhuber, U. Meier, and D. Ciresan, "Multi-column deep neural networks for image classification," in *Proc. IEEE Conf. Comput. Vis. Pattern Recognit.*, 2012, pp. 3642–3649.
[20] D. Amodei *et al.*, "Deep speech 2: End-to-end speech recognition in English and mandarin," in *Proc. Int. Conf. Mach. Learn.*, 2016, pp. 173–182.
[21] Y. Ganin *et al.*, "Domain-adversarial training of neural networks," *J. Mach. Learn. Res.*, vol. 17, no. 59, pp. 1–35, 2016.
[22] H. Hinrikus *et al.*, "Electroencephalographic spectral asymmetry index for detection of depression," *Med. Biol. Eng. Comput.*, vol. 47, no. 12, p. 1291, 2009.
[23] Y. Li, W. Zheng, Y. Zong, Z. Cui, T. Zhang, and X. Zhou, "A bi-hemisphere domain adversarial neural network model for EEG emotion recognition," *IEEE Trans. Affect. Comput.*, early access, Dec. 7, 2018, doi: 10.1109/TAFFC.2018.2885474.
[24] Y. Li, W. Zheng, Z. Cui, Y. Zong, and S. Ge, "EEG emotion recognition based on graph regularized sparse linear regression," *Neural Process. Lett.*, vol. 49, pp. 1–17, Apr. 2018.
[25] T. Zhang, W. Zheng, Z. Cui, Y. Zong, and Y. Li, "Spatial–temporal recurrent neural network for emotion recognition," *IEEE Trans. Cybern.*, vol. 49, no. 3, pp. 839–847, Mar. 2019.
[26] T. Song, W. Zheng, P. Song, and Z. Cui, "EEG emotion recognition using dynamical graph convolutional neural networks," *IEEE Trans. Affect. Comput.*, early access, Mar. 21, 2018, doi: 10.1109/TAFFC.2018.2817622.
[27] T. Song, W. Zheng, C. Lu, Y. Zong, X. Zhang, and Z. Cui, "MPED: A multi-modal physiological emotion database for discrete emotion recognition," *IEEE Access*, vol. 7, pp. 12177–12191, 2019.
[28] L. Bottou, "Large-scale machine learning with stochastic gradient descent," in *Proc. COMPSTAT*, 2010, pp. 177–186.
[29] J. A. Suykens and J. Vandewalle, "Least squares support vector machine classifiers," *Neural Process. Lett.*, vol. 9, no. 3, pp. 293–300, 1999.
[30] L. Breiman, "Random forests," *Mach. Learn.*, vol. 45, no. 1, pp. 5–32, 2001.
[31] B. Thompson, "Canonical correlation analysis," in *Encyclopedia of Statistics in Behavioral Science*. Chichester, U.K.: Wiley, 2005.
[32] M. Defferrard, X. Bresson, and P. Vandergheynst, "Convolutional neural networks on graphs with fast localized spectral filtering," in *Proc. Adv. Neural Inf. Process. Syst. (NIPS)*, 2016, pp. 3844–3852.
[33] Y. Li, W. Zheng, Z. Cui, T. Zhang, and Y. Zong, "A novel neural network model based on cerebral hemispheric asymmetry for EEG emotion recognition," in *Proc. Int. Joint Conf. Artif. Intell. (IJCAI)*, 2018, pp. 1561–1567.
[34] W.-L. Zheng and B.-L. Lu, "Personalizing EEG-based affective models with transfer learning," in *Proc. Int. Joint Conf. Artif. Intell. (IJCAI)*, 2016, pp. 2732–2738.
[35] M. Sugiyama, S. Nakajima, H. Kashima, P. V. Buenau, and M. Kawanabe, "Direct importance estimation with model selection and its application to covariate shift adaptation," in *Proc. Adv. Neural Inf. Process. Syst. (NIPS)*, 2008, pp. 1433–1440.
[36] T. Kanamori, S. Hido, and M. Sugiyama, "A least-squares approach to direct importance estimation," *J. Mach. Learn. Res.*, vol. 10, pp. 1391–1445, Jul. 2009.
[37] W.-S. Chu, F. De la Torre, and J. F. Cohn, "Selective transfer machine for personalized facial expression analysis," *IEEE Trans. Pattern Anal. Mach. Intell.*, vol. 39, no. 3, pp. 529–545, Mar. 2017.
[38] S. J. Pan, I. W. Tsang, J. T. Kwok, and Q. Yang, "Domain adaptation via transfer component analysis," *IEEE Trans. Neural Netw.*, vol. 22, no. 2, pp. 199–210, Feb. 2011.
[39] B. Fernando, A. Habrard, M. Sebban, and T. Tuytelaars, "Unsupervised visual domain adaptation using subspace alignment," in *Proc. IEEE Int. Conf. Comput. Vis. (ICCV)*, 2013, pp. 2960–2967.
[40] B. Gong, Y. Shi, F. Sha, and K. Grauman, "Geodesic flow kernel for unsupervised domain adaptation," in *Proc. IEEE Conf. Comput. Vis. Pattern Recognit. (CVPR)*, 2012, pp. 2066–2073.
[41] H. Li, Y.-M. Jin, W.-L. Zheng, and B.-L. Lu, "Cross-subject emotion recognition using deep adaptation networks," in *Proc. Int. Conf. Neural Inf. Process.*, 2018, pp. 403–413.
[42] W.-L. Zheng, J.-Y. Zhu, and B.-L. Lu, "Identifying stable patterns over time for emotion recognition from EEG," *IEEE Trans. Affective Comput.*, vol. 10, no. 3, pp. 417–429, Jul.–Sep. 2019.
[43] G. Chanel, J. J. Kierkels, M. Soleymani, and T. Pun, "Short-term emotion assessment in a recall paradigm," *Int. J. Human–Comput. Stud.*, vol. 67, no. 8, pp. 607–627, 2009.
[44] M. Balconi and G. Mazza, "Brain oscillations and BIS/BAS (behavioral inhibition/activation system) effects on processing masked emotional cues: ERS/ERD and coherence measures of alpha band," *Int. J. Psychophysiol.*, vol. 74, no. 2, pp. 158–165, 2009.
[45] Y. Liu, O. Sourina, and M. K. Nguyen, "Real-time EEG-based emotion recognition and its applications," in *Transactions on Computational Science XII*. Berlin, Germany: Springer, 2011, pp. 256–277.
[46] N. Jatupaiboon, S. Pan-Ngum, and P. Israsena, "Emotion classification using minimal EEG channels and frequency bands," in *Proc. IEEE 10th Int. Joint Conf. Comput. Sci. Softw. Eng. (JCSSE)*, 2013, pp. 21–24.
[47] D. Huang, C. Guan, K. K. Ang, H. Zhang, and Y. Pan, "Asymmetric spatial pattern for EEG-based emotion detection," in *Proc. IEEE Int. Joint Conf. Neural Netw. (IJCNN)*, 2012, pp. 1–7.
[48] J. A. Coan and J. J. Allen, "Frontal EEG asymmetry as a moderator and mediator of emotion," *Biol. Psychol.*, vol. 67, nos. 1–2, pp. 7–50, 2004.
[49] M. Davis and P. J. Whalen, "The amygdala: Vigilance and emotion," *Mol. Psychiatry*, vol. 6, no. 1, p. 13, 2001.

Yang Li (Member, IEEE) received the B.S. degree in electronic information and science technology from the School of Physics and Electronics, Shandong Normal University, Jinan, China, in 2012, the M.S. degree in electronic and communication engineering from the School of Electronic Engineering, Xidian University, Xi'an, China, in 2015, and the Ph.D. degree from the School of Information Science and Engineering, Southeast University, Nanjing, China, in 2020.

He was also a visiting student with the University of Wollongong, Wollongong, NSW, Australia, from August 2018 to August 2019. He is currently an Associate Professor with the School of Artificial Intelligence, Xidian University. His research interests focus on affective computing, pattern recognition, and computer vision.

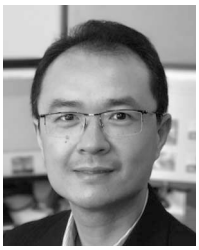

Lei Wang (Senior Member, IEEE) received the Ph.D. degree from Nanyang Technological University, Singapore, in 2004.

He is currently an Associate Professor with the School of Computing and Information Technology, University of Wollongong, Wollongong, NSW, Australia. He has published over 160 peer-reviewed papers, including those in highly regarded journals and conferences, such as the IEEE TRANSACTIONS ON PATTERN ANALYSIS AND MACHINE INTELLIGENCE, the *International Journal of Computer Vision*, CVPR, ICCV, and ECCV. His research interests include machine learning, pattern recognition, and computer vision.

Dr. Wang was awarded the Early Career Researcher Award by Australian Academy of Science and Australian Research Council. He served as the General Co-Chair of DICTA 2014 and the Program Co-Chair of VCIP2019 and will serve as the Program Co-Chair of ACCV2022.

Wenming Zheng (Senior Member, IEEE) received the B.S. degree in computer science from Fuzhou University, Fuzhou, China, in 1997, the M.S. degree in computer science from Huaqiao University, Quanzhou, China, in 2001, and the Ph.D. degree in signal processing from Southeast University, Nanjing, China, in 2004.

Since 2004, he has been with the Research Center for Learning Science, Southeast University, where he is currently a Professor with the School of Biological Science and Medical Engineering and the Key Laboratory of Child Development and Learning Science, Ministry of Education. His current research interests include affective computing, pattern recognition, machine learning, and computer vision.

Prof. Zheng served as an Associate Editor for several peer-reviewed journals, such as the IEEE TRANSACTIONS ON AFFECTIVE COMPUTING, *Neurocomputing*, and *Visual Computer*.

Yuan Zong (Member, IEEE) received the B.S. and M.S. degrees in electronics engineering from Nanjing Normal University, Nanjing, China, in 2011 and 2014, respectively, and the Ph.D. degree in biomedical engineering from Southeast University, Nanjing, in 2018.

He is currently a Lecturer with the Key Laboratory of Child Development and Learning Science of Ministry of Education, School of Biological Science and Medical Engineering, Southeast University. From 2016 to 2017, he was a visiting student with the Center for Machine Vision and Signal Analysis, University of Oulu, Oulu, Finland. He has published over 20 papers in mainstream journals and conferences, such as the IEEE TRANSACTIONS ON IMAGE PROCESSING, the IEEE TRANSACTIONS ON CYBERNETICS, the IEEE TRANSACTIONS ON AFFECTIVE COMPUTING, AAAI, IJCAI, and ACM MM. His research interests include affective computing, pattern recognition, and computer vision.

Lei Qi is currently pursuing the Ph.D. degree with the Department of Computer Science and Technology, Nanjing University, Nanjing, China.

He was also a visiting student with the University of Wollongong, Wollongong, NSW, Australia, from August 2018 to August 2019. For applications, he mainly focuses on person reidentification and image segmentation. He is currently interested in some ML methods, such as domain adaptation, semisupervised learning, unsupervised learning, and meta learning.

Zhen Cui (Member, IEEE) received the Ph.D. degree from the Institute of Computing Technology, Chinese Academy of Sciences, Beijing, China, in 2014.

He was a Research Fellow with the Department of Electrical and Computer Engineering, National University of Singapore, Singapore, from 2014 to 2015. He also spent half a year as a Research Assistant with Nanyang Technological University, Singapore, from June 2012 to December 2012. He is currently a Professor with the Nanjing University of Science and Technology, Nanjing, China. He has published several papers in the top conferences NIPS/CVPR/ECCV and some journals of IEEE transactions. His research interests cover computer vision, pattern recognition, and machine learning, especially focusing on deep learning, manifold learning, sparse coding, face detection/alignment/recognition, object tracking, image super resolution, and emotion analysis. More details can be found in http://aip.seu.edu.cn/zcui/.

Tong Zhang (Member, IEEE) received the B.S. degree from the School of Information Science and Engineering, Southeast University, Nanjing, China, in 2011, the M.S. degree from the Research Center for Learning Science, Southeast University in 2014, and the Ph.D. degree from the School of Information Science and Engineering, Southeast University in 2018.

He is currently a Lecturer with the School of Computer Science and Engineering, Nanjing University of Science and Technology, Nanjing. His current research interests include pattern recognition, machine learning, and computer vision.

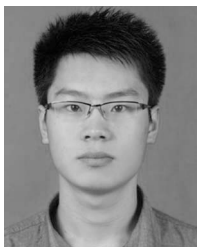

Tengfei Song (Member, IEEE) received the B.S. degree in communication engineering from Hohai University, Jiangsu, China, in 2016. He is currently pursuing the Ph.D. degree with the Department of Information and Communication Engineering, Southeast University, Nanjing, China.

His research interests include affective computing, computer vision, machine learning, and pattern recognition.